Analysis and Prediction of Printable Bridge Length in Fused Deposition Modelling Based on Back Propagation Neural Network

Jingchao Jiang[1], Guobiao Hu[1], Xiao Li[2], Xun Xu[1], Pai Zheng[3], Jonathan Stringer[1]

[1]*Department of Mechanical Engineering, University of Auckland, New Zealand*

[2]*Department of Design, National Taiwan University of Science and Technology, Taiwan*

[3]*School of Mechanical and Aerospace Engineering, Nanyang Technological University, Singapore 639798, Singapore*

Abstract

In recent years, the additive manufacturing technology has been developed rapidly mainly due to the ease of fabricating complex components. However, complex structures with overhangs inevitably require support materials to prevent collapse and reduce warping of the part. In this paper, the effects of process parameters on printable bridge length (PBL) are investigated. An optimization is conducted to maximize the distance between support points, thus minimizing the support usage. The orthogonal design method is employed for designing the experiments. The samples are then used to train a neural network for predicting the nonlinear relationships between PBL and process parameters. The results show that the established neural network can correctly predict the longest PBL which can be integrated into support generation process in additive manufacturing for maximizing the distance between support points, thus reducing support usage. A framework for integrating the findings of this paper into support generation process is proposed.

Keywords: Additive manufacturing; Support; Printable bridge length; Back propagation neural network.

1. Introduction

The technology of 3D printing which is also often termed as additive manufacturing (AM) was first developed in 1987 by 3D Systems (Wohlers and Gornet 2014). Due to the rapid development, it has already had a wide of applications in the fields of aerospace, medical application and personalized products (Zheng et al. 2017; Weng, Li, Tan, et al. 2018; C. Wang et al. 2018; Weng, Li, Liu, et al. 2018; Li et al. 2016). Different from traditional manufacturing technologies by cutting material away from a solid block of material, AM techniques construct 3D objects by successively depositing material in layers such that it becomes the predesigned shape. When there are substantial overhanging structures, the layer-by-layer depositing nature of AM may result in a consequence that the current layer cannot be deposited successfully if without the assistance of some additional supports underneath (Leary et al. 2014; Jiang, Stringer, and Xu 2018; Jiang, Xu,

and Stringer 2018). For this reason, support structures are often required to be generated additionally for a large group of AM techniques except some powder-based AM processes for which the fully self-support can be realized by the powders. Moreover, after manufacturing, objects have to be post-processed by manually removing the support structures. Therefore, it can be understood that the existence of the support structures causes the waste of materials, increases the time for production and cost for post-processing.

In the past few years, immense interests have been attracted to improve AM to become a more economical, sustainable and environmental-friendly technique. David et al. (2018) analysed potential environmental implications of AM related to energy consumption, occupational health, waste and lifecycle impact. An approach for the design of experiments was developed by Griffiths et al. (2016) for reducing the waste and energy during the AM process. Improving or even developing new AM technologies for reducing cost is also an attractive research field (McElheny, Hayes, and Devireddy 2017). In terms of the extrusion-based AM technology, the team of Jin has carried out lots of research (Jin, Du, Ma, et al. 2017; Jin, Du, and He 2017; Jin, He, et al. 2017; Jin, Du, He, et al. 2017) to optimize the process planning for the purpose of reducing production time, material and energy.

In the AM process, support structure is another important source of waste as they only serve for manufacturing assistance and have to be removed after fabrication. Studies for reducing supports have also been conducted by many researchers (Li et al. 2017; Mumtaz, Vora, and Hopkinson 2011; Strano et al. 2013; Barnett and Gosselin 2015; Gaynor and Guest 2016; Jiang, Stringer, Xu, and Zheng 2018; Zhang et al. 2017). Generally speaking, all these works are based on three methods: optimizing build orientation to avoid the requirements of support structures, using cheaper material to generate support structures, and seeking better support structures (e.g. cellular/lattice structures). Besides the methods proposed above, another potential way to reduce the support waste is by adjusting the process parameters for increasing the printable distance between support points, thus decreasing the demand of support structures. For example, on the premise of ensuring a satisfied quality, a bridge may be printed without using any support beneath it (see Fig. 1(a)), or maybe at least two support points (see Fig. 1(b)), or maybe three points (see Fig. 1(c)). The number of the required supporting points depends on the longest distance a 3D printer can print which is affected by various process parameters. There are many studies (Chowdhury, Mhapsekar, and Anand 2017; Armillotta, Bellotti, and Cavallaro 2018; G. Dong et al. 2018) working on investigating the effects of process parameters on the printed surface quality including roughness and deformation etc. Mohamed et al. (Mohamed, Masood, and Bhowmik

2016) optimized the process parameters for dimensional accuracy using I-optimality criterion in FDM processes. Jiang et al. (2018a) studied the effects of process parameters on the threshold of the printable overhang angle and determined the lowest angle that can be printed through tuning the process parameters.

In this paper, the effects of process parameters (including print speed, cooling fan speed and print temperature) on the printable bridge length (PBL) are investigated for an FDM printer. The orthogonal method is employed for designing 32 tests of experiments with different process parameters. Subsequently, a back propagation neural network (BPNN) is trained based on that set of experimental sample data to establish the nonlinear relationship between PBL and process parameters. After that, process parameters are optimized for achieving the longest printable distance which means the longest bridge a 3D printer can print (with satisfied finish surface quality) without using any additional support structure (see Fig. 1(a)). The feature and results of the longest PBL can be integrated into slicers for slicing 3D models and generating supports, thus minimizing support usage and production cost in future printing processes. Then the longest PBL can be predicted by the established BPNN. Finally, characters "UOA" and pane parts are fabricated vertically according to the longest PBL predicted by BPNN for validation.

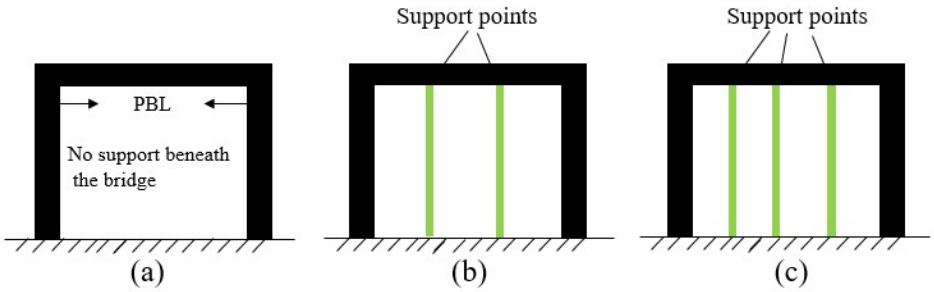

Fig. 1 Concepts of support point and PBL (green struts are support structures); (a) Bridge does not need support for getting qualified result; (b) Bridge needs two support points; (c) Bridge needs three support points.

2. Physical analysis

During an AM process, there are many factors (print temperature, print speed, cooling fan speed, etc.) that may influence PBL. Some works have been carried out for achieving the longest PBL from a design perspective (Rosen 2014; Lischke and Tovar 2016). In this section, the effect of main factors (print speed, cooling fan speed and print temperature) on PBL will be analysed in a physical perspective.

2.1 Effect of print speed on PBL

Print speed is an important factor that can influence PBL. Imaging a printing process as shown in Fig. 2, once the print speed (i.e., the moving speed of the nozzle) is low enough, the extruded

material (that beneath the nozzle) is supposed to have enough time to be solidified before the nozzle moves to next point of printing. The higher the print speed is, the more the melted material is out of the nozzle within a unit time and the more time it takes to solidify the melted material, resulting in larger collapse/deformation. In this case, theoretically speaking, PBL could be in any length once the print speed is low enough. However, the printed material may still be in molten phase even the print speed is zero, because the print nozzle keeps at a high temperature and there must exist heat transfer between the nozzle and the printed material. Therefore, in a real printing process, PBL has a threshold influenced by print speed. The exact relationship between PBL and print speed will be studied by experiments and BPNN in the following sections.

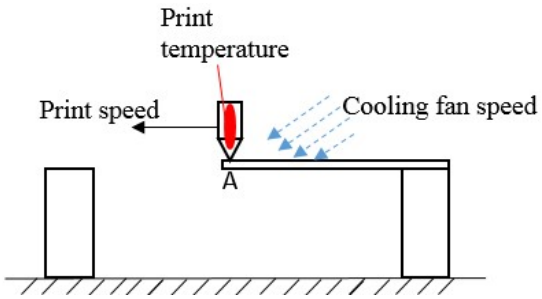

Fig. 2 Illustration of effects of process parameters

2.2 Effect of cooling fan speed on PBL

Cooling fan speed is closely related to the solidification speed of printed material and thus is another important factor of PBL. As can be seen in Fig. 2, when the cooling fan speed becomes higher, the time for printed material to become solid will be less, leading to smaller deformation. Theoretically speaking, the faster the solidification speed is, the longer the PBL could be. In a printing process, cooling fan speed, environmental temperature and air condition will all have influences on the solidification process. Among these factors, cooling fan speed is the primary factor as the others stay almost the same and are not as influential as cooling fan speed. The exact relationship between PBL and cooling fan speed will be studied by experiments and BPNN in the following sections.

2.3 Effect of print temperature on PBL

Print temperature is also a significant factor. In this study, print temperature is seen the same as the temperature inside the print nozzle (chamber) during a printing process. Higher print temperature means higher temperature of melted material, resulting in longer time for a printed material to become solid and may lead to larger deformation. The exact relationship between PBL and print temperature will be studied by experiments and BPNN in the following sections.

As analysed above, PBL can be theoretically influenced by print speed, print temperature and cooling fan speed. As shown in the literature, the printed strength/solidity/quality can also be influenced by all the process parameters (Decuir, Phelan, and Hollins 2016; Pfeifer et al. 2016). For satisfying the requirements of a product, the process parameters have to be certain in a range. For example, if the strength of a product is required to be high enough, the print temperature needs to be higher than some threshold. In this case, the longest PBL should be tested for saving material, production time and cost. BPNN will be trained and used for predicting the longest PBL and providing an optimal process parameter combination. Once the process parameters of a fabrication process are set as required, the longest PBL will be able to be predicted and can be integrated into a slicing software for generating less support, reducing production time and prime cost.

3. Experimental study

The equipment used for manufacturing parts is a Kossel Delta 3D printer. The effects of print temperature, print speed and cooling fan speed on PBL were tested by using this printer. The build area shape is circular with diameter of 180 mm and maximum height of 300 mm. The nozzle diameter of this equipment is 0.4 mm. The material used for fabrication is Polylactic Acid (PLA).

3.1 Bridge design

The objective of this research is to achieve the longest PBL under an optimal process parameter combination. Hence, bridge with lengths of 1, 2, 3, 4, 5 and 6 mm was designed by using the commercial CAD software Solidworks to observe their corresponding deformations. 2D and 3D views of designed bridge part are displayed in Fig. 3 with dimensions. the thickness of this bridge is 1 mm. In order to use the characteristics of the longest PBL for reducing support waste in the future, the print path pattern has to be as shown in Fig. 4(a). Print path in this pattern can achieve the longest print distance without any support, based on the longest PBL. This is because of the printing nature of 3D printing. As shown in Fig. 4(c), if the print path is in a vertical pattern rather than horizontal, there will be no support points beneath the ends of each print path which will lead to collapse because of the layer by layer nature of AM (Jiang, Lou and Hu, 2019).

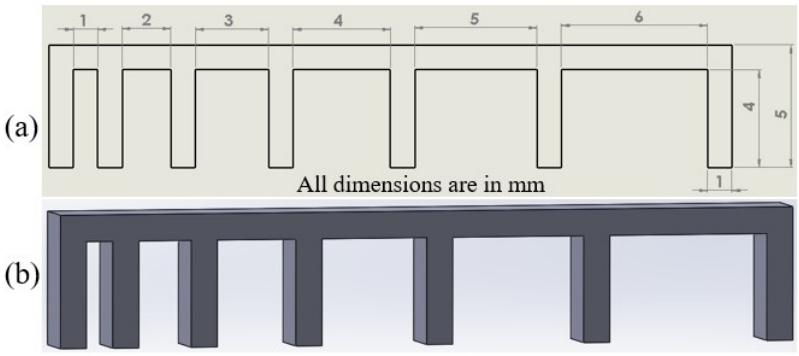

Fig. 3 (a) 2D view of bridge (Unit: mm); (b) 3D view of bridge

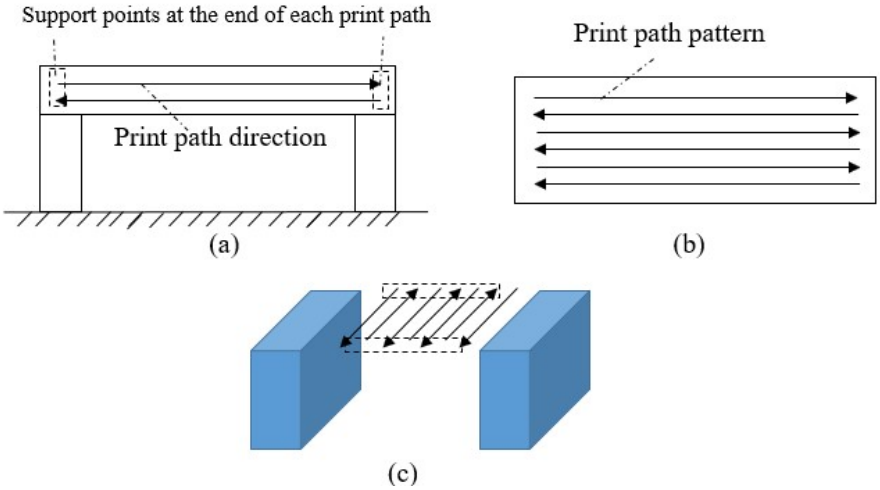

Fig.4 (a) Front view of print path; (b) Top view of print path pattern; (c) No support points beneath the ends of each print path, this is unprintable

3.2 Design of experiments (DOE)

The design of experiments (DOE) is a tool to obtain experimental information by using statistical methods. The principles of DOE include randomization, blocking, replication and orthogonality. Based on those principles, factorial experimental design has been proposed to obtain extensive information from only a few sets of experiments compared with the one factor at a time method (OFAT). As a branch of factorial experimental design, the orthogonal design has been extensively used in various fields as a kind of multi-level, high-efficiency and economical test method (Zurovac and Brown 2012). In the orthogonal design, the effect of many factors and some of their interactions can be studied simultaneously in a single set of experiments with much fewer experiment units. An orthogonal analysis (OA) needs to be chosen in the first place. In this study, the OA of L32 was chosen because it can be used to study four factors (bridge length, print speed, print temperature and cooling fan speed), among them bridge length has six levels and every remaining factor has four levels.

The L32 OA with four columns and 32 experimental runs is shown in Table 1 with the same other process parameters (0.2 mm of layer height, 0.8 mm of shell thickness, 1mm of bottom/top thickness and 20% of fill density). Slicer software Cura 15.04 was used for slicing digital models.

Table 1 Orthogonal design matrix

Runs	Bridge length (mm)	Print Speed (mm/s)	Print Temperature (°C)	Cooling Fan Speed (RPM)
1	1	65	205	0
2	1	35	205	85
3	1	5	220	0
4	1	65	190	170
5	1	5	175	170
6	1	95	220	85
7	1	35	190	255
8	1	95	175	255
9	2	35	175	85
10	2	5	205	170
11	2	65	175	0
12	2	95	205	255
13	2	65	220	170
14	2	5	190	0
15	2	95	190	85
16	2	35	220	255
17	3	65	175	255
18	3	35	220	0
19	3	5	205	85
20	3	95	190	170
21	4	95	220	170
22	4	65	205	255
23	4	35	190	0
24	4	5	175	85
25	5	95	205	0
26	5	65	220	85
27	5	5	190	255
28	5	35	175	170
29	6	35	205	170
30	6	95	175	0
31	6	65	190	85
32	6	5	220	255

3.3 Results

After obtaining the printed parts, image-based analysis was carried out as the procedure shown in Fig. 5(a). Specifically, each photo of the printed geometry was analysed by NI vision assistant in conjunction with Engauge Digitizer. In the analysis process, only the largest deformation under each condition was measured based on the bottom contour as shown in Fig. 5(b). The reason of

taking the largest deformation for comparison is that the quality of a product is determined by the largest deformation which should be within tolerance. All these 32 experiments were carried out 5 times repeatedly. For each experiment, the average value of five runs under the same condition is chosen as the final data in avoid of random error. The corresponding results are shown in Table 2.

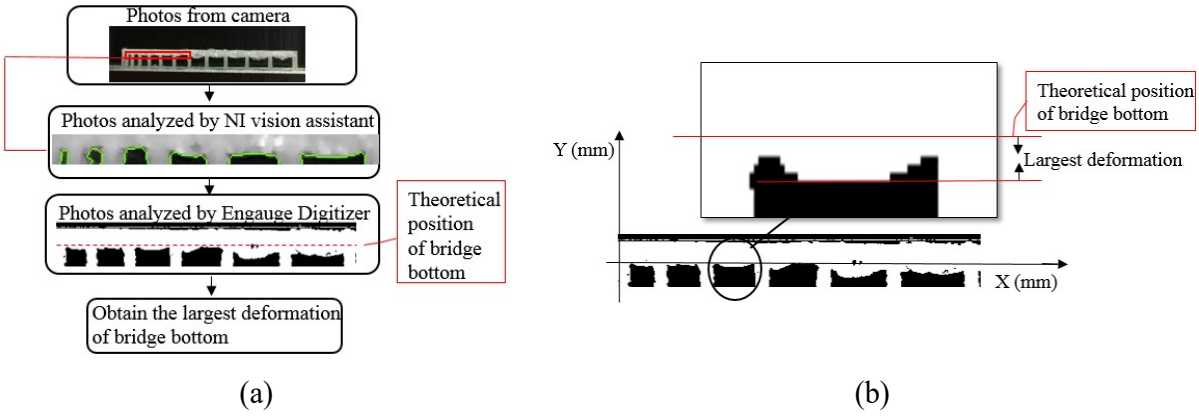

Fig. 5 (a) Analysis program of bridges; (b) Definition of largest deformation in these bridges

Table 2 Range of largest deformations in each experiment in different runs

Runs	1	2	3	4	5	6	7	8
Largest deformation (mm)	0.138-0.142	0.105-0.111	0.106-0.113	0.101-0.109	0.059-0.065	0.148-0.154	0.075-0.078	0.102-0.106
Runs	9	10	11	12	13	14	15	16
Largest deformation (mm)	0.188-0.192	0.156-0.160	0.251-0.253	0.239-0.243	0.242-0.247	0.193-0.196	0.271-0.279	0.179-0.186
Runs	17	18	19	20	21	22	23	24
Largest deformation (mm)	0.349-0.353	0.521-0.524	0.366-0.371	0.499-0.506	1.398-1.415	1.027-1.033	1.155-1.160	0.770-0.778
Runs	25	26	27	28	29	30	31	32
Largest deformation (mm)	2.114-2.127	1.811-1.817	0.790-0.797	1.100-1.107	1.302-1.307	1.919-1.927	1.611-1.617	0.989-0.997

4. BP neural Network for predicting PBL and analysis

Relationships between PBL and various process parameters are uncertain and may involve nonlinearities. It is difficult to develop an analytical model which involves the multidisciplinary parameters related to the complicated process to predict the printed quality. Therefore, an approximate model based on the data fitting technique is needed for addressing this issue. The fitting quality of the conventional polynomial regression method strongly depends on the selection of polynomial form which often requires a quite good precognition of the relationships between

input and output parameters. An artificial neural network (ANN) is a computational model based on the biologically inspired structure and functions. ANNs are well-known powerful tools for prediction of nonlinearities and have wide applications in various areas such as pattern recognition, system identification, and nonlinear function fitting and intelligent control. The BP model is applied widely because of its simplicity and robustness (Jiang et al. 2014; Wang et al. 2011; Dong, Lian, and Liu 2018). In the field of AM, Noriega et al. (2013) investigated dimensional accuracy improvement of FDM square cross-section parts using ANN. For enhancing surface roughness of FDM parts, Vahabli and Rahmati (2016; 2017) used neural network to predict the surface quality of printed parts. Chowdhury et al. (2017) tried to adopt neural network to make appropriate geometric modifications in AM processes for improving printed surface quality. Chowdhury and Anand (2016) also did some research on thermal deformation in AM processes via ANN. In addition, the effects of process parameters on creep and recovery behaviour of FDM manufactured part were studied by Mohamed et al. (2017) based on ANN. In this paper, neural network will also be applied for studying process parameters' effects on PBL and predicting the longest PBL.

4.1 BPNN structure

The structure of a general BP neural network is shown in Fig. 6, including three layers: input layer, hidden layer and output layer. The input neurons are indirectly connected to the output neurons through hidden neurons. The connection between two neurons has a weight property to represent the relation degree. The establishment of a BPNN model includes determining the number of input and output neurons, selecting the number of neurons to be used in hidden layer and determining weight values of connections. There are many different algorithms for training neural networks. The back-propagation (BP) algorithm is currently the most widely used one. The mechanism of BP algorithm can be briefly described as follows. At the first stage, the inputs propagate forward and the output is generated. At the second stage, the error between the generated and actual outputs is calculated and backward propagated to the input layer, then the weights on connections are accordingly changed to reduce the error. This process of adjusting the connection weights is repeatedly performed until the resulting network fits the training data well i.e., errors between the predicted and actual outputs are sufficiently small.

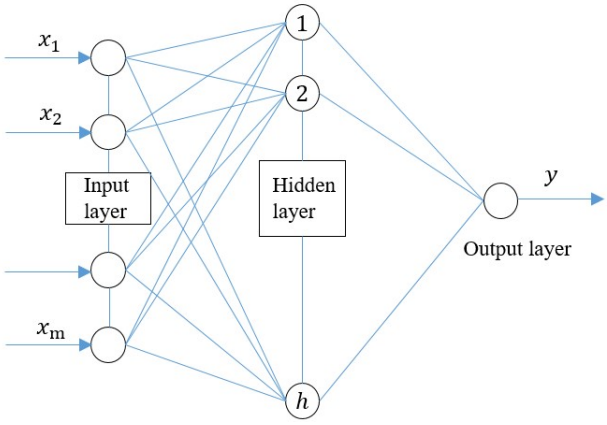

Fig. 6 Structure of a general BP neural network

4.2 Establishment of BPNN model

The implementation of a BPNN model consists of selecting the number neurons in input and output layers, determining the number of neurons in hidden layer and determining weight values of connections. The number of input neurons is 4 and corresponding inputs are print speed, cooling fan speed, print temperature and bridge length. There is only one output neuron which corresponds to deformation of bridge bottom in different situations. Though there is no method to accurately calculate the optimal number of hidden layer neurons, based on experience, the following formula can be referred in designing (Tian 2009).

$$h=\sqrt{m+n}+a \tag{1}$$

in which h is the number of hidden layer neurons, m is the number of input layer neurons, n is the number of output layer neurons, a is the constant between 1 to 10. To achieve best fitting performance, a is varied to minimize the forecast error.

The weight values of connections are ceaselessly adjusted during the process of training until the prediction errors are reduced below a certain threshold. The training samples are selected by using the orthogonal experimental design method which features uniform dispersion and neat comparison. The sample value ranges are listed in Table 3.

Table 3 Sample value ranges

Factors	Parameters	Range
1	Bridge length (mm)	1~6
2	Print Speed (mm/s)	5~95
3	Print Temperature (℃)	175~220
4	Cooling Fan Speed (RPM)	0~255

The training sample data has been given out in the previous section. In order to ensure the convergence, the sample data is normalized with a formula as follows:

$$y_i = \frac{x_i - \min(x_i)}{\max(x_i) - \min(x_i)} \tag{2}$$

where, x_i and y_i are the original and the normalized data of the *i*-th input, respectively; $\max(x_i)$ and $\min(x_i)$ are the maximum and minimum in the sample of the *i*-th input, respectively. After the normalization process, the data is re-ranged between 0 and 1.

4.3 Performance evaluation

The Neural Network Training toolbox built in the commercial software Matlab is used for developing the neural network. The Bayesian Regularization algorithm is selected as the learning method, due to its robustness. Fig. 7(a) shows the mean squared error (MSE) during the training process. It can be seen that after 54 iterations the value of MSE reaches minimum and remains almost constant. Fig. 7(b) demonstrates the prediction performance by comparing the targeted actual outputs and the predicted outputs. It can be concluded that the developed BPNN model shows a high accuracy for predicting the relationships between the input and the output parameters.

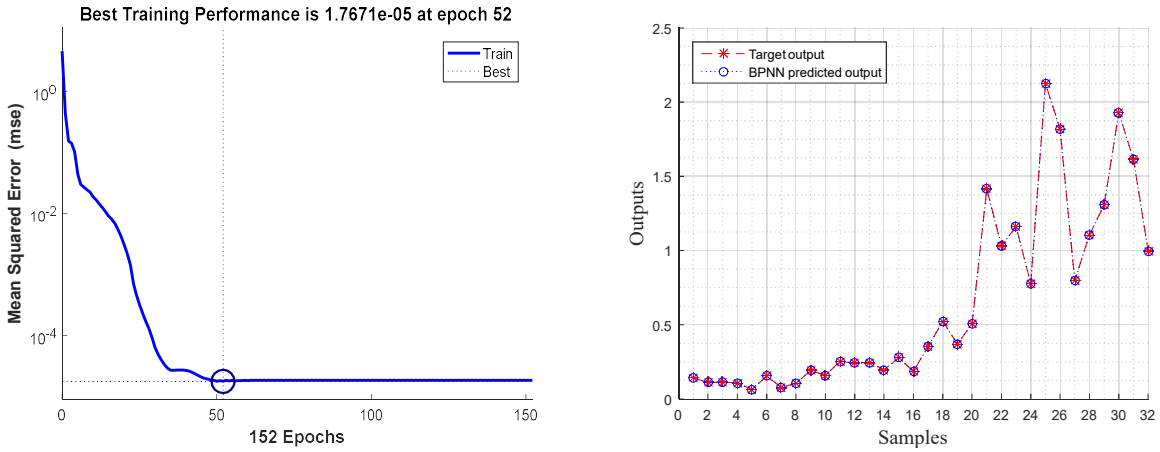

(a) (b)

Fig. 7 (a) Mean squared error during the training process; (b) Prediction performance

4.4 Factor analysis

Based on the trained BPNN model, effects of the four input parameters on the output, i.e., deformation, are investigated. For given two parameters and by varying the other two parameters, Fig. 8 shows the variations of the largest deformations. Constant values are selected for factor analysis as follows: bridge length is set at 2 mm; print speed at 30 mm/s; print temperature at 205 °C and cooling fan speed at 255 RPM.

From Fig. 8(a), (d) and (c), it can be seen that the largest deformation increases as the increase of print speed. This is because the higher the print speed is, the more the melted material is out of the

nozzle and there is less time for the melted material to solidify, resulting in a larger deformation. As can be seen from Fig. 8(a), (b) and (c), the largest deformation increases significantly with the increase of the bridge length. The main purpose of this research is to predict the largest PBL under certain conditions i.e., for given process parameters. From Fig. 8(b), (d) and (f), it is noted that with the increase of print temperature, the largest deformation increases. As illustrated in the section of physical analysis, the increase of print temperature leads to the increase of time required for the melted material to be solidified. Therefore, if all other process parameters are kept the same, a larger deformation will be formed as print temperature increases. From Fig. 8(c), (e) and (f), it is noted that with the increase of cooling fan speed, the largest deformation decreases. The fan is used to cool the melted material and fasten its solidification speed. Reasonably, the higher the cooling fan speed is, the faster the melted material solidifies, resulting in a smaller deformation.

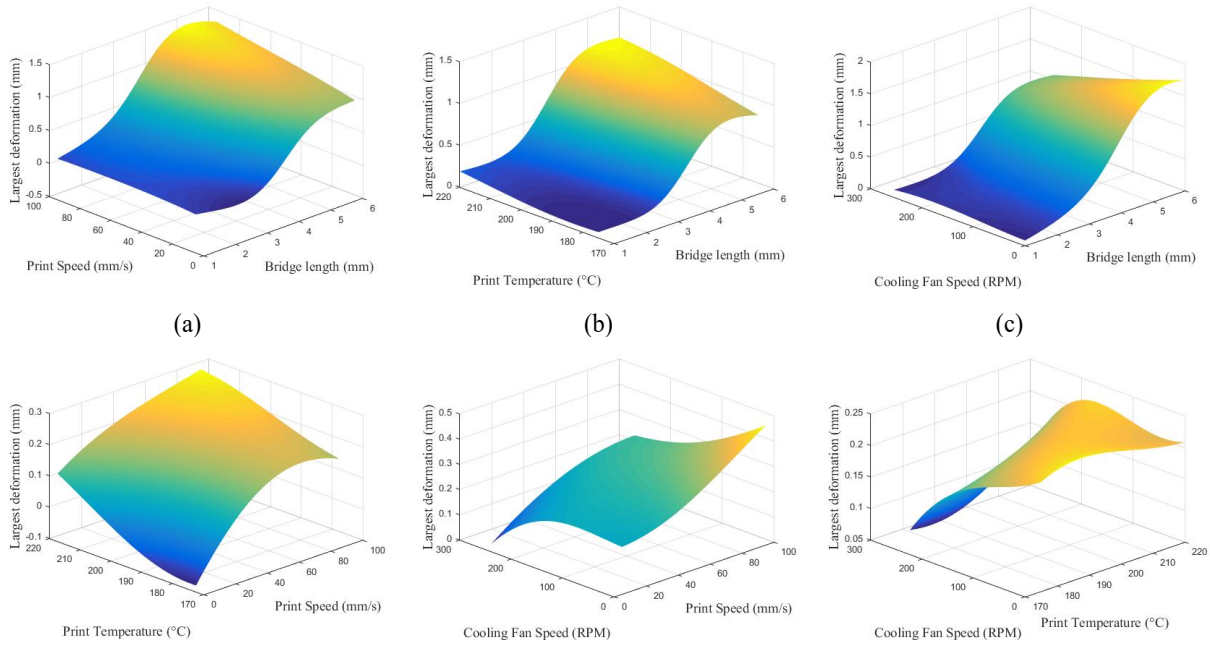

Fig. 8 Variations of the largest deformations in different conditions

However, it is noteworthy that in some regions of some figures, the relationships between the input and the output parameters do not absolutely follow the tendencies as concluded above. For example, in Fig. 8(d), when the print temperature is low, with the increase of print speed, the deformation first increases (as expected) then decreases against prediction. In Fig. 8(f), when the cooling fan speed is low, with the increase of print temperature, the deformation is not monotonously increasing as predicted. However, these errors only rarely occur when the bridge length is small. The bridge length for both cases in Figs. 8(d) and (f) is 2 mm. The reason of the prediction error is mainly due to the initial measurement errors. When the bridge length is small,

the deformation itself is comparatively very small regardless of other process parameters. Thus the variations between those deformations of bridges may be too small to be accurately predicted by BPNN, as compared with the counterparts with large bridge lengths. While considering the aim of this research is to predict the longest PBL rather than focusing on the small bridge lengths, the BPNN is reasonably acceptable for being used to predict the longest PBL.

Overall, the effects of process parameters on the largest deformation are in good accordance with physical explanations. This also indicates that the developed BPNN model can well predict the relationships between the process parameters and the largest deformation of printed bridges. To further intuitively verify the above predictions of the relationships between the input and output parameters, several comparative experiments were carried out. The predicted effects of the four parameters on the largest deformation of printed bridges are confirmed as shown in Fig. 9. Figs. 9(g) and (h) compare the actual and predicted largest deformations of these samples. It can be observed that the deformation trend predicted from the ANN model matches the actual result: with the increase of the bridge length, the bridge is more prone to deform. Both the actual and predicted results show that the overall deformation of sample (a) is the smallest. This is because that the print speed for sample (a) is the lowest. Recalling that the print speed has a significant effect on the printed quality: with the increase of the print speed, the bridge is more easily to deform, this result is physically expectable. Coincidently but also as expected, both the actual and predicted results show that the overall deformation of sample (e) is the largest. This may be explained by the highest print temperature for sample (e). However, one can observe some deviations between Fig. 9 (g) and (h). For example, for sample (c), according to the prediction from the ANN model, with the increase of the bridge length the deformation should monotonously increases. Whereas, the actual result is that the deformation first increases then decreases (which can also be macroscopically observed in Fig.9 (c)). Unfortunately, the reasonable physical explanation is not found for the abnormal case. It is speculated that this may be related to the reliability of the machine used in the research. Besides that one can note that for sample (e), the prediction error is significant, especially when the bridge length becomes larger than 5 mm. The explanation for the generation of this significant prediction error is that for sample (e) (Fig. 9(e)), when the bridge length is larger than 5 mm, the deformation becomes extremely large and already exceeds the largest deformation of the training samples. It implies that this sample is beyond the cognition scope of the developed ANN model. Therefore, the developed ANN model fails to provide an accurate prediction for sample (e). Overall speaking, the developed ANN model shows a good prediction ability.

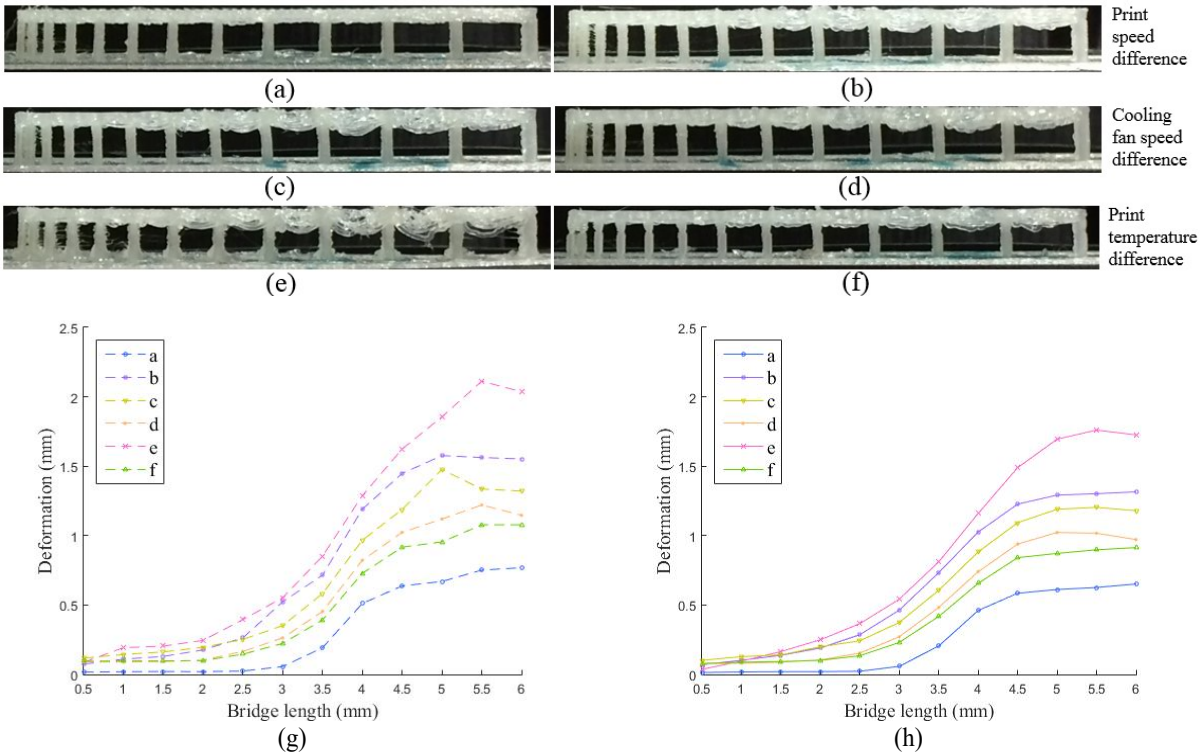

Fig. 9 Samples printed in different conditions; (a) Part printed in print speed of 5 mm/s, cooling fan speed of 250 RPM, print temperature of 190 ℃; (b) Part printed in print speed of 95 mm/s, cooling fan speed of 250 RPM, print temperature of 190 ℃; (c) Part printed in cooling fan speed of 0 RPM, print speed of 35 mm/s, print temperature of 190 ℃; (d) Part printed in cooling fan speed of 250 RPM, print speed of 35 mm/s, print temperature of 190 ℃; (e) Part printed in print temperature of 220 ℃, cooling fan speed of 250 RPM, print speed of 35 mm/s; (f) Part printed in print temperature of 175 ℃,cooling fan speed of 250 RPM, print speed of 35 mm/s. (g) Largest deformations of the samples shown in (a)-(f). (h) Corresponding predictions from the developed ANN model for the samples shown in (a)-(f).

5. Conceptual framework for practical applications

As illustrated above, BPNN is able to correctly predict the longest PBL which can then be integrated into support generation process in additive manufacturing processes for maximizing the distance between support points and subsequently minimizing the support usage. In the future, once the requirements of process parameters are available, BPNN can then be used to get the longest PBL for generating supports before fabricating a targeted object. The framework for reducing future support consumption based on process parameter requirements and BPNN is shown in Fig. 10.

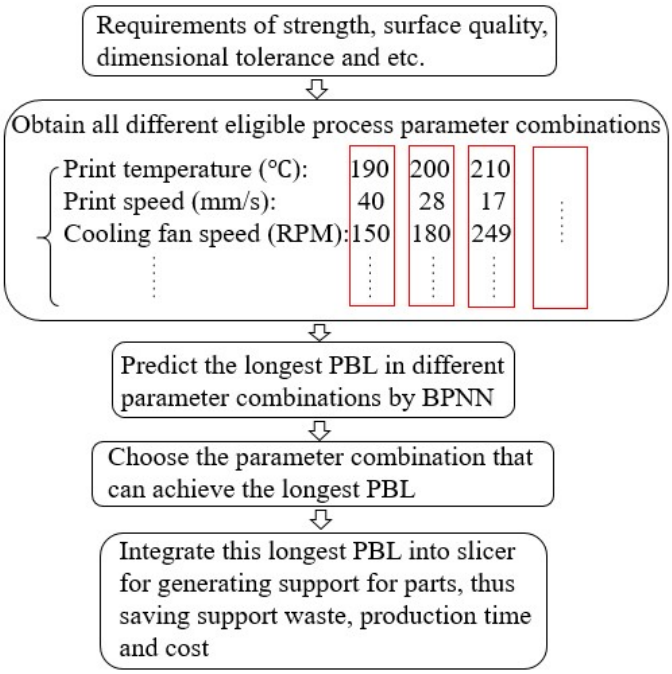

Fig. 10 Framework of using BPNN for reducing support waste in additive manufacturing processes

Figure 11 shows some examples printed with very clear bridge structures for clearly demonstrating deformation results, according to the longest PBL predicted by BPNN. The process parameters required are as follows: print temperature of 190 ℃, print speed of 30 mm/s and cooling fan speed of 255RPM. The largest deformation within tolerance is set as 0.2 mm. Based on the above requirements, the longest PBL predicted by BPNN is 2.8 mm. For ensuring the printed quality, 80% of the predicted length (i.e. 2.2 mm) of PBL is designed in all the parts having bridge features in Fig. 11. All the bridge deformations are less than 0.2 mm, with satisfied finishes after printing.

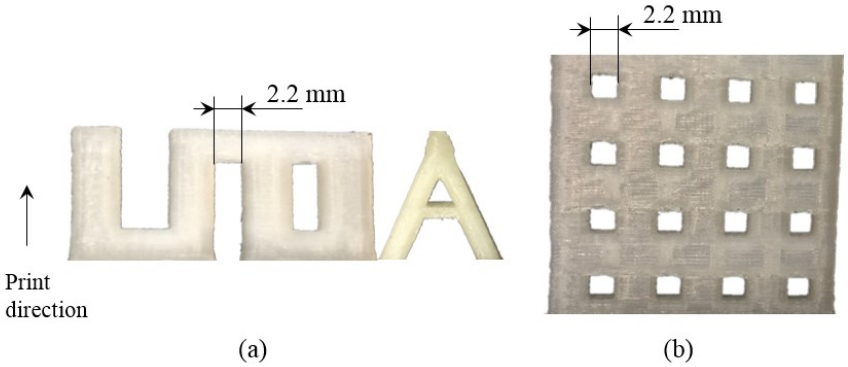

Fig. 11 Printed “UOA” and pane parts with satisfied bridge deformations (thickness of these parts is 2 mm)

6. Conclusions

In this paper, process parameters' effects on PBL are investigated for achieving the longest PBL, thus maximizing the distance between support points and subsequently minimizing the support usage. Orthogonal design is employed for setting 32 tests of experiments in different process parameters as neural network training sample to establish the nonlinear relationship between PBL and process parameters. The relationships between process parameters and PBL are studied based on BPNN. The findings and methods in this paper can also be used for future high-precision additive manufacturing. The main contributions of this paper can be made as follows:

- The effects of process parameters on PBL are studied for the first time for improving the printable distance. Based on the experiments, the longest PBL can be increased as print temperature decreases, cooling fan speed increases and print speed decreases.
- The results show that BPNN can correctly predict the longest PBL which can be integrated into support generation process in additive manufacturing processes for maximizing the distance between support points, thus reducing support usage. The longest PBL predicted by BPNN is 2.8 mm when setting the largest deformation tolerance at 0.2 mm, print temperature at 190 ℃, print speed at 30 mm/s and cooling fan speed at 255 RPM. "UOA" and pane parts were fabricated with PBL of 2.2 mm and shows satisfied finfish quality.
- Artificial neural networks are used to analyse and predict PBL for optimizing the support waste in additive manufacturing processes. A framework for future application on reducing support waste is proposed as shown in Fig. 10.

References

Armillotta, Antonio, Mattia Bellotti, and Marco Cavallaro. 2018. "Warpage of FDM Parts: Experimental Tests and Analytic Model." *Robotics and Computer-Integrated Manufacturing* 50 (April). Pergamon: 140–152. doi:10.1016/J.RCIM.2017.09.007.

Barnett, Eric, and Clément Gosselin. 2015. "Weak Support Material Techniques for Alternative Additive Manufacturing Materials." *Additive Manufacturing* 8: 95–104. doi:10.1016/j.addma.2015.06.002.

Chowdhury, Sushmit, and Sam Anand. 2016. "Artificial Neural Network Based Geometric Compensation for Thermal Deformation in Additive Manufacturing Processes." In *Volume 3: Joint MSEC-NAMRC Symposia*, V003T08A006. ASME. doi:10.1115/MSEC2016-8784.

Chowdhury, Sushmit, Kunal Mhapsekar, and Sam Anand. 2017. "Part Build Orientation Optimization and Neural Network-Based Geometry Compensation for Additive Manufacturing Process." *Journal of Manufacturing Science and Engineering* 140 (3). American Society of Mechanical Engineers: 031009. doi:10.1115/1.4038293.

David, Rejeski, Zhao Fu, and Huang Yong. 2018. "Research Needs and Recommendations on Environmental Implications of Additive Manufacturing." *Additive Manufacturing* 19

(January). Elsevier: 21–28. doi:10.1016/J.ADDMA.2017.10.019.

Decuir, Francois, Kelsey Phelan, and Bryant C. Hollins. 2016. “Mechanical Strength of 3-D Printed Filaments.” In *2016 32nd Southern Biomedical Engineering Conference (SBEC)*, 47–48. IEEE. doi:10.1109/SBEC.2016.101.

Dong, Guoying, Grace Wijaya, Yunlong Tang, and Yaoyao Fiona Zhao. 2018. “Optimizing Process Parameters of Fused Deposition Modeling by Taguchi Method for the Fabrication of Lattice Structures.” *Additive Manufacturing* 19 (January). Elsevier: 62–72. doi:10.1016/J.ADDMA.2017.11.004.

Dong, X., Y. Lian, and Y. Liu. 2018. “Small and Multi-Peak Nonlinear Time Series Forecasting Using a Hybrid Back Propagation Neural Network.” *Information Sciences* 424. doi:10.1016/j.ins.2017.09.067.

Gaynor, Andrew T., and James K. Guest. 2016. “Topology Optimization Considering Overhang Constraints: Eliminating Sacrificial Support Material in Additive Manufacturing through Design.” *Structural and Multidisciplinary Optimization* 54 (5): 1157–1172. doi:10.1007/s00158-016-1551-x.

Griffiths, C. A., J. Howarth, G. De Almeida-Rowbotham, A. Rees, and R. Kerton. 2016. “A Design of Experiments Approach for the Optimisation of Energy and Waste during the Production of Parts Manufactured by 3D Printing.” *Journal of Cleaner Production* 139: 74–85. doi:10.1016/j.jclepro.2016.07.182.

Jiang, Jingchao, Jonathan Stringer, Xun Xu, and Pai Zheng. 2018. “A Benchmarking Part for Evaluating and Comparing Support Structures of Additive Manufacturing.” In *3rd International Conference on Progress in Additive Manufacturing (Pro-AM 2018)*, 196–202. doi:10.25341/D42G6H.

Jiang, Jingchao, Jonathan Stringer, Xun Xu, and Ray Y. Zhong. 2018a. “Investigation of Printable Threshold Overhang Angle in Extrusion-Based Additive Manufacturing for Reducing Support Waste.” *International Journal of Computer Integrated Manufacturing* 31 (10): 961–969. doi:10.1080/0951192X.2018.1466398.

Jiang, Jingchao, Xun Xu, and Jonathan Stringer. 2018. “Support Structures for Additive Manufacturing: A Review.” *Journal of Manufacturing and Materials Processing, 2(4):64*. doi:10.3390/JMMP2040064.

Jiang, Jngchao, Jonathan Stringer, and Xun Xu. 2018. “Support Optimization for Flat Features via Path Planning in Additive Manufacturing.” *3D Printing and Additive Manufacturing*. doi:10.1089/3dp.2017.0124.

Jiang, Jingchao, Jingjun Lou, and Guobiao Hu. 2019. “Effect of Support on Printed Properties in Fused Deposition Modelling Processes.” *Virtual and Physical Prototyping*. doi:10.1080/17452759.2019.1568835.

Jiang, Z., Y. Liu, H. Chen, and Q. Hu. 2014. “Optimization of Process Parameters for Biological 3D Printing Forming Based on BP Neural Network and Genetic Algorithm.” In *Advances in Transdisciplinary Engineering*, 351–358. doi:10.3233/978-1-61499-440-4-351.

Jin, Yuan, Jianke Du, and Yong He. 2017. “Optimization of Process Planning for Reducing Material Consumption in Additive Manufacturing.” *Journal of Manufacturing Systems* 44 (July). Elsevier: 65–78. doi:10.1016/J.JMSY.2017.05.003.

Jin, Yuan, Jianke Du, Yong He, and Guoqiang Fu. 2017. “Modeling and Process Planning for Curved Layer Fused Deposition.” *International Journal of Advanced Manufacturing Technology* 91 (1–4). The International Journal of Advanced Manufacturing Technology:

273–285. doi:10.1007/s00170-016-9743-5.

Jin, Yuan, Jianke Du, Zhiyong Ma, Anbang Liu, and Yong He. 2017. “An Optimization Approach for Path Planning of High-Quality and Uniform Additive Manufacturing.” *International Journal of Advanced Manufacturing Technology* 92 (1–4). The International Journal of Advanced Manufacturing Technology: 651–662. doi:10.1007/s00170-017-0207-3.

Jin, Yuan, Yong He, Guoqiang Fu, Aibing Zhang, and Jianke Du. 2017. “A Non-Retraction Path Planning Approach for Extrusion-Based Additive Manufacturing.” *Robotics and Computer-Integrated Manufacturing* 48 (December 2016). Elsevier Ltd: 132–144. doi:10.1016/j.rcim.2017.03.008.

Leary, Martin, Luigi Merli, Federico Torti, Maciej Mazur, and Milan Brandt. 2014. “Optimal Topology for Additive Manufacture: A Method for Enabling Additive Manufacture of Support-Free Optimal Structures.” *Materials and Design* 63: 678–690. doi:10.1016/j.matdes.2014.06.015.

Li, Mingyang et al. 2016. “Modeling and Analysis of Paste Freezing in Freeze-Form Extrusion Fabrication of Thin-Wall Parts via a Lumped Method.” *Journal of Materials Processing Technology* 237 (November): 163–180. doi:10.1016/j.jmatprotec.2016.05.027

Li, Zhonghua, David Zhengwen Zhang, Peng Dong, and Ibrahim Kucukkoc. 2017. “A Lightweight and Support-Free Design Method for Selective Laser Melting.” *The International Journal of Advanced Manufacturing Technology* 90 (9–12). Springer London: 2943–2953. doi:10.1007/s00170-016-9509-0.

Lischke, F, and A Tovar. 2016. “Design of Self-Supported 3D Printed Parts for Fused Deposition Modeling.” In *Proceedings of the ASME 2016 International Design Engineering Technical Conferences and Computers and Information in Engineering Conference* , 1–8. Charlotte, North Carolina . http://risk.asmedigitalcollection.asme.org/pdfaccess.ashx?resourceid=13841019&pdfsource=13.

McElheny, Colton, Daniel Hayes, and Ram Devireddy. 2017. “Design and Fabrication of a Low-Cost Three-Dimensional Bioprinter.” *Journal of Medical Devices* 11 (4): 041001. doi:10.1115/1.4037259.

Mohamed, Omar Ahmed, Syed Hasan Masood, and Jahar Lal Bhowmik. 2016. “Optimization of Fused Deposition Modeling Process Parameters for Dimensional Accuracy Using I-Optimality Criterion.” *Measurement* 81 (March). Elsevier: 174–196. doi:10.1016/J.MEASUREMENT.2015.12.011.

Mohamed, Omar Ahmed, Syed Hasan Masood, and Jahar Lal Bhowmik. 2017. “Influence of Processing Parameters on Creep and Recovery Behavior of FDM Manufactured Part Using Definitive Screening Design and ANN.” *Rapid Prototyping Journal* 23 (6). Emerald Publishing Limited : 998–1010. doi:10.1108/RPJ-12-2015-0198.

Mumtaz, K.A., P. Vora, and N. Hopkinson. 2011. “A Method to Eliminate Anchors/Supports from Directly Laser Melted Metal Powder Bed Processes.” In *Solid Freeform Fabrication Symposium*. Sheffield. http://eprints.whiterose.ac.uk/103245/.

Noriega, A., D. Blanco, B. J. Alvarez, and A. Garcia. 2013. “Dimensional Accuracy Improvement of FDM Square Cross-Section Parts Using Artificial Neural Networks and an Optimization Algorithm.” *The International Journal of Advanced Manufacturing Technology* 69 (9–12). Springer London: 2301–2313. doi:10.1007/s00170-013-5196-2.

Pfeifer, Thomas, Carsten Koch, Luke Van Hulle, Gerardo A Mazzei Capote, and Natalie Rudolph. 2016. “OPTIMIZATION OF THE FDM™ ADDITIVE MANUFACTURING PROCESS.”

In *Proceedings of the Annual Technical Conference (ANTEC) of the Society of Plastics Engineers*, 22–29. Indianapolis. http://leaders.4spe.org/spe/conferences/antec2016/papers/235.pdf.

Rosen, David W. 2014. "Research Supporting Principles for Design for Additive Manufacturing." *Virtual and Physical Prototyping* 9 (4). Taylor & Francis: 225–232. doi:10.1080/17452759.2014.951530.

Strano, G., L. Hao, R. M. Everson, and K. E. Evans. 2013. "A New Approach to the Design and Optimisation of Support Structures in Additive Manufacturing." *International Journal of Advanced Manufacturing Technology* 66 (9–12): 1247–1254. doi:10.1007/s00170-012-4403-x.

Tian Yubo. 2009. "Hybrid neural network technology." Beijing: Science Press.

Vahabli, Ebrahim, and Sadegh Rahmati. 2016. "Application of an RBF Neural Network for FDM Parts' Surface Roughness Prediction for Enhancing Surface Quality." *International Journal of Precision Engineering and Manufacturing* 17 (12). Korean Society for Precision Engineering: 1589–1603. doi:10.1007/s12541-016-0185-7.

Vahabli, Ebrahim, and Sadegh Rahmati. 2017. "Improvement of FDM Parts' Surface Quality Using Optimized Neural Networks – Medical Case Studies." *Rapid Prototyping Journal* 23 (4). Emerald Publishing Limited : 825–842. doi:10.1108/RPJ-06-2015-0075.

Wang, Chengcheng, Xipeng Tan, Erjia Liu, and Shu Beng Tor. 2018. "Process Parameter Optimization and Mechanical Properties for Additively Manufactured Stainless Steel 316L Parts by Selective Electron Beam Melting." *Materials & Design* 147 (June). Elsevier: 157–166. doi:10.1016/J.MATDES.2018.03.035.

Wang, Jian Zhou, Ju Jie Wang, Zhe George Zhang, and Shu Po Guo. 2011. "Forecasting Stock Indices with Back Propagation Neural Network." *Expert Systems with Applications* 38 (11): 14346–14355. doi:10.1016/j.eswa.2011.04.222.

Weng, Yiwei, Mingyang Li, Zhixin Liu, Wenxin Lao, Bing Lu, Dong Zhang, and Ming Jen Tan. 2018. "Printability and Fire Performance of a Developed 3D Printable Fibre Reinforced Cementitious Composites under Elevated Temperatures." *Virtual and Physical Prototyping*, December. Taylor & Francis, 1–9. doi:10.1080/17452759.2018.1555046.

Weng, Yiwei, Mingyang Li, Ming Jen Tan, and Shunzhi Qian. 2018. "Design 3D Printing Cementitious Materials via Fuller Thompson Theory and Marson-Percy Model." *Construction and Building Materials* 163: 600–610. doi:10.1016/j.conbuildmat.2017.12.112.

Wohlers, Terry, and Tim Gornet. 2014. "History of Additive Manufacturing." *Wohlers Report 2014 - 3D Printing and Additive Manufacturing State of the Industry*, 1–34. doi:10.1017/CBO9781107415324.004.

Zhang, Yicha, Alain Bernard, Ramy Harik, and K. P. Karunakaran. 2017. "Build Orientation Optimization for Multi-Part Production in Additive Manufacturing." *Journal of Intelligent Manufacturing* 28 (6): 1393–1407. doi:10.1007/s10845-015-1057-1.

Zheng, Pai, Yuanbin Wang, Xun Xu, and Sheng Quan Xie. 2017. "A Weighted Rough Set Based Fuzzy Axiomatic Design Approach for the Selection of AM Processes." *The International Journal of Advanced Manufacturing Technology* 91 (5–8). Springer London: 1977–1990. doi:10.1007/s00170-016-9890-8.

Zurovac, J, and Randy Brown. 2012. "Orthogonal Design: A Powerful Method for Comparative Effectiveness Research with Multiple Interventions." *Center on Healthcare Effectiveness, ...*, no. April. http://www.mathematica-

mpr.com/publications/PDFs/health/orthogonaldesign_ib.pdf.